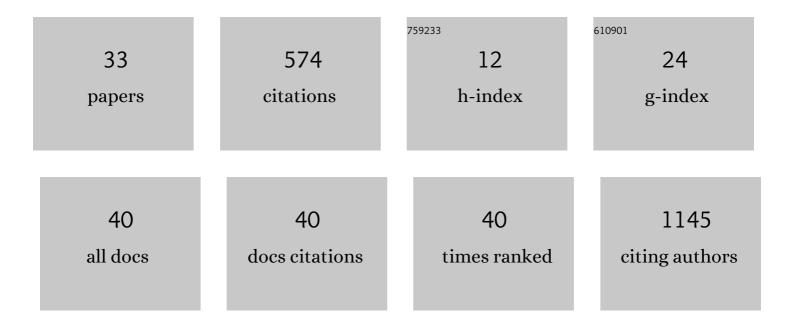
## Vadim Migunov

List of Publications by Year in descending order

Source: https://exaly.com/author-pdf/5409086/publications.pdf Version: 2024-02-01



6

#	Article	IF	CITATIONS
1	Experimental and Theoretical Understanding of Nitrogen-Doping-Induced Strong Metal–Support Interactions in Pd/TiO <sub>2</sub> Catalysts for Nitrobenzene Hydrogenation. ACS Catalysis, 2017, 7, 1197-1206.	11.2	138
2	Electron Microscopy (Big and Small) Data Analysis With the Open Source Software Package HyperSpy. Microscopy and Microanalysis, 2017, 23, 214-215.	0.4	74
3	Rapid low dose electron tomography using a direct electron detection camera. Scientific Reports, 2015, 5, 14516.	3.3	71
4	Atomic-scale quantification of charge densities in two-dimensional materials. Physical Review B, 2018, 98, .	3.2	36
5	Model-independent measurement of the charge density distribution along an Fe atom probe needle using off-axis electron holography without mean inner potential effects. Journal of Applied Physics, 2015, 117, .	2.5	30
6	Automated discrete electron tomography– Towards routine high-fidelity reconstruction of nanomaterials. Ultramicroscopy, 2017, 175, 87-96.	1.9	27
7	LiberTEM: Software platform for scalable multidimensional data processing in transmission electron microscopy. Journal of Open Source Software, 2020, 5, 2006.	4.6	26
8	Planar-defect characteristics and cross-sections of ã€^001〉, ã€^111〉, and ã€^112〉 InAs nanowires. Jo Physics, 2011, 109, 114320.	ournal of Ap	oplied
9	Tunable caustic phenomena in electron wavefields. Ultramicroscopy, 2015, 157, 57-64.	1.9	20
10	Fabrication and characterization of a focused ion beam milled lanthanum hexaboride based cold field electron emitter source. Applied Physics Letters, 2018, 113, 093101.	3.3	17
11	<i>In situ</i> transmission electron microscopy of resistive switching in thin silicon oxide layers. Resolution and Discovery, 2016, 1, 27-33.	0.4	16
12	Operando Transmission Electron Microscopy Study of All-Solid-State Battery Interface: Redistribution of Lithium among Interconnected Particles. ACS Applied Energy Materials, 2020, 3, 5101-5106.	5.1	14
13	Prospects for quantitative and time-resolved double and continuous exposure off-axis electron holography. Ultramicroscopy, 2017, 178, 48-61.	1.9	12
14	Tunable Ampere phase plate for low dose imaging of biomolecular complexes. Scientific Reports, 2018, 8, 5592.	3.3	11
15	Effect of preparation of iron-infiltrated activated carbon catalysts on nitrogen oxide conversion at low temperature. Applied Catalysis B: Environmental, 2014, 160-161, 641-650.	20.2	9
16	Measurement of charge density in nanoscale materials using off-axis electron holography. Journal of Electron Spectroscopy and Related Phenomena, 2020, 241, 146881.	1.7	9
17	Quantitative measurement of charge accumulation along a quasi-one-dimensional W <sub>5</sub> O <sub>14</sub> nanowire during electron field emission. Nanoscale, 2020, 12, 10559-10564.	5.6	7

18Three-dimensional electric field mapping of an electrically biased atom probe needle using off-axis<br/>electron holography. Microscopy and Microanalysis, 2019, 25, 326-327.0.4

VADIM MIGUNOV

#	Article	IF	CITATIONS
19	Enhancement of magneto-optical response in nanocomposite-hydrogenated amorphous silicon multilayers. Bulletin of the Russian Academy of Sciences: Physics, 2008, 72, 1379-1381.	0.6	5
20	Continuous illumination picosecond imaging using a delay line detector in a transmission electron microscope. Ultramicroscopy, 2022, 233, 113392.	1.9	5
21	Imaging At the Timescale Of Micro- and Milliseconds With the pnCCD (S)TEM Camera. Microscopy and Microanalysis, 2015, 21, 1585-1586.	0.4	4
22	Single Electron Precision in the Measurement of Charge Distributions on Electrically Biased Graphene Nanotips Using Electron Holography. Nano Letters, 2019, 19, 4091-4096.	9.1	4
23	Dense, Regular GaAs Nanowire Arrays by Catalyst-Free Vapor Phase Epitaxy for Light Harvesting. ACS Applied Materials & Interfaces, 2016, 8, 22484-22492.	8.0	2
24	Live Measurement of Electrical Charge Density in Materials using Off-Axis Electron Holography. Microscopy and Microanalysis, 2019, 25, 44-45.	0.4	2
25	<i>Operando</i> transmission electron microscopy of battery cycling: thickness dependent breaking of TiO <sub>2</sub> coating on Si/SiO <sub>2</sub> nanoparticles. Chemical Communications, 2022, 58, 3130-3133.	4.1	2
26	New Approaches for Measuring Electrostatic Potentials and Charge Density Distributions in Working Devices Using Off-Axis and In-Line Electron Holography. Microscopy and Microanalysis, 2014, 20, 260-261.	0.4	1
27	Electron Holography of the Magnetic Phase Shift of a Current-Carrying Wire. Microscopy and Microanalysis, 2014, 20, 278-279.	0.4	1
28	Measurement of Atomic Electric Fields by Scanning Transmission Electron Microscopy (STEM) Employing Ultrafast Detectors. Microscopy and Microanalysis, 2016, 22, 484-485.	0.4	1
29	Electron Transport in Partially Filled Iron Carbon Nanotubes. Solid State Phenomena, 2012, 190, 498-501.	0.3	0
30	Electric and Magnetic Field Mapping With the pnCCD (S)TEM Camera. Microscopy and Microanalysis, 2016, 22, 256-257.	0.4	0
31	Pushing the Limits of Fast Acquisition in TEM Tomography and 4D-STEM. Microscopy and Microanalysis, 2016, 22, 512-513.	0.4	0
32	Model-Based Iterative Reconstruction of Charge Density in Nanoscale Materials using Off-Axis Electron Holography. Microscopy and Microanalysis, 2019, 25, 48-49.	0.4	0
33	Three-dimensional Charge Density and Electric Field Mapping of an Electrically Biased Needle Using Off-axis Electron Holography. Microscopy and Microanalysis, 2020, 26, 1540-1542.	0.4	0